

Effect of boundary conditions on modal parameters of the Run Yang Suspension Bridge

Zhijun Li^{*1a}, Aiqun Li^{1b} and Jian Zhang^{2c}

¹College of Civil Engineering, Southeast University, Nanjing 210096, P.R. China

²Department of Civil Engineering, National University of Singapore, Singapore 117576

(Received April 23, 2009, Accepted December 15, 2009)

Abstract. Changes in temperature, loads and boundary conditions may have effects on the dynamic properties of large civil structures. Taking the Run Yang Suspension Bridge as an example, modal properties obtained from ambient vibration tests and from the structural health monitoring system of the bridge are used to identify and evaluate the modal parameter variability. Comparisons of these modal parameters reveal that several low-order modes experience a significant change in frequency from the completion of the bridge to its operation. However, the correlation analysis between measured modal parameters and the temperature shows that temperature has a slight influence on the low-order modal frequencies. Therefore, this paper focuses on the effects of the boundary conditions on the dynamic behaviors of the suspension bridge. An analytical model is proposed to perform a sensitivity analysis on modal parameters of the bridge concerning the stiffness of expansion joints located at two ends of bridge girders. It is concluded that the boundary conditions have a significant influence on the low-order modal parameters of the suspension bridge. In addition, the influence of vehicle load on modal parameters is also investigated based on the proposed model.

Keywords: suspension bridge; ambient vibration test; structural health monitoring system; boundary condition; expansion joints.

1. Introduction

Dynamic performance and vibration characteristics of suspension bridges have been concerns of researchers in bridge engineering. Despite of huge advances in numerical modeling of civil engineering structures in recent decades, finite element models for suspension bridges should be developed and used with caution when evaluating modal properties of these structures. This is due to some inherent modeling uncertainties related to a lack of information of the as-built structures, such as boundary conditions, material properties and the influences of non-structural elements. From the point of view of structural health monitoring, it is extremely important to discriminate changes in the structural behavior due to damage from changes by environmental and operational fluctuations (Ko *et al.* 2003, Sohn *et al.* 1999). Combination of experimental test and numerical analysis is helpful to better understand the structural vibration behavior and to provide key information for safety assessments.

*Corresponding Author, PhD Candidate, E-mail: civil_lizj@yahoo.com.cn

^aPhD Candidate

^bProfessor

^cResearch Fellow

Ambient vibration tests would facilitate the identification of dynamic characteristics, e.g., natural frequencies, damping ratios and mode shapes, which are the basis for validating and/or updating analytical models of the structure. It corresponds to the real operating condition of the bridge, and has been successfully applied to several large scale cable-supported bridges (Fujino and Siringoringo 2007, Ren *et al.* 2004).

Technologies of structural health monitoring for surveillance, evaluation and assessment of existing or newly built bridges have become mature in recent years. On-structure long-term monitoring systems have been implemented on bridges in Europe, United States, Canada, Japan, Korea, China and some other countries (Ko and Ni 2005). The dynamic responses of bridges can be successfully measured with the structural health monitoring system installed on the bridge. Using these data, various system identification approaches are applied independently to detect the potential changes in vibration characteristics.

The Run Yang Suspension Bridge (RYSB) over the Yangtze River is a super long suspension bridge in China. At the center of the main span, the main cables and the steel box girder are connected by the rigid central nodes, which are used for the first time in China to improve the fatigue behaviors of short suspenders. To understand the structural dynamic behavior, several ambient vibration tests have been conducted to obtain the modal parameters during the construction of the bridge. Meanwhile, vibration information collected by the bridge health monitoring system are used to identify modal parameters at different times, such as before and after the bridge opened to traffic and in typhoon. Comparison of the identified modal frequencies of the bridge at different times reveals that some low-order modal frequencies actually experience significant variations. The effects of temperature, vehicle loads and boundary conditions are taken into account to interpret the variations. Known from the correlation analysis between measured modal parameters and the temperature, ambient temperature only has a slight influence on the low-order modal frequencies. Therefore, this paper focuses on the effect of boundary conditions on the dynamic behaviors of the RYSB.

This paper is organized as follows. First, modal parameters measured by ambient vibration tests during different construction stages of the bridge are presented, followed by the introduction to the structural health monitoring system of the RYSB. Some cases of modal parameters obtained from the system are presented and compared. Modal parameters in different temperatures are statistically analyzed. Thereafter, the effects of boundary conditions and vehicle load on modal parameters are discussed based on a three-dimensional finite element model. Finally, conclusions of this study are drawn.

2. Run Yang Suspension Bridge

The Run Yang Suspension Bridge, as shown in Fig. 1, is the longest bridge in China when it was open to traffic in 2005. The bridge has a main span of 1490 m and two symmetric side spans of 470 m. The central span consists of a streamlined steel box girder.

The main cables and suspenders are made of prefabricated parallel wire strands with diameters of 0.9 m and 0.07 m, respectively. The towers, about 210 m tall, are made of prestressed concrete. Tower foundations consist of two pile caps (21.6×21.6 m) and 16 piles with a diameter of 2.8 m and a length of about 60 m. The construction of the bridge was started in 2000 and ended in December 2004. It was finally opened to traffic on May 1st, 2005.



Fig. 1 Run Yang Suspension Bridge

3. Ambient vibration test

Ambient vibration test has recently become one of the main experimental methods for assessing the dynamic behaviors of full-scale structures, especially for flexible systems such as suspension and cable-stayed bridges (Fujino and Siringoringo 2007, Magalhaes *et al.* 2008, Gentil and Gallino 2008). Ambient vibration testing techniques are based on the so-called ‘output-only’ modal identification, which is capable of extracting modal parameters using output-only responses. The operational modal identification has been carried out in the frequency domain using the classic peak picking (PP) method and the frequency domain decomposition (FDD) method (Brincker *et al.* 2001, He *et al.* 2009).

3.1 Peak picking method

A basic step of this method is the evaluation of spectral estimates of the ambient structural responses from the measured time series. The main steps can be illustrated as follows:

- 1) Calculate the auto-spectral density (ASD) or power-spectral density (PSD) of all measured points and obtain an average normalized power spectral density function (ANPSD). The natural frequencies can be identified in terms of spectral peak response (peak picking).
- 2) Calculate mode shape and damping of all orders.

In fact, for a lightly damped structure subjected to a white noise random excitation, both ASD and cross-spectral density (CSD) reach a local maximum at the frequencies corresponding to the structural normal modes. The ratio of square root of the ASD at different points can be considered as an estimate of amplitude of mode shapes. The real part of the CSD indicates whether the points are moving in the same sense (zero phase values) or in the opposite senses (π rad phase values). In the context of the PP method, the identification of modal damping coefficients is usually performed using the half-power bandwidth method, but the result is not reliable.

3.2 Frequency domain decomposition method

Another modal estimation method adopted in this study is called ‘frequency domain decomposition (FDD)’.

The output PSD matrix $G_{yy}(j\omega)$ can be expressed as

$$G_{yy}(j\omega) = \bar{H}(j\omega)\hat{G}_{xx}(j\omega)H(j\omega)^T \quad (1)$$

where $G_{xx}(j\omega)$ is the PSD matrix of the input, $H(j\omega)$ is the frequency response function (FRF) and the overbar and superscript T denote the complex conjugate and transpose, respectively.

Assume the input is white noise, then the input PSD matrix is a constant matrix ($G_{xx}(j\omega)=C$). Substituting the FRF matrix with the pole/residue form into Eq. (1), the output PSD matrix will be reduced to a pole/residue form. Then in the controlling field of a certain modal frequency ω , the output PSD matrix can be written as

$$G_{yy}(j\omega) \approx \phi_k \text{diag} \left[2\text{Re} \left(\frac{d_k}{j\omega - \lambda_k} \right) \right] \cdot \bar{\phi}_k^T \quad (2)$$

where d_k is a scalar constant, ϕ_k and λ_k are the mode shape vector and k th pole, respectively.

In the FDD identification, the first step is to estimate PSD matrix $\hat{G}_{yy}(j\omega)$ from the measurements and then decomposed at discrete frequencies $\omega = \omega_i$ by taking singular value decomposition (SVD) of the matrix

$$\hat{G}_{yy}(j\omega_i) = U_i S_i U_i^T \quad (3)$$

where the matrix $U_i = [u_{i1}, u_{i2}, \dots, u_{im}]$ is a unitary matrix holding the singular vector u_{ij} , and S_i is a diagonal matrix holding the scalar singular values s_{ij} .

It is observed from Eqs. (2) and (3) that when the frequency approaches a modal frequency ω_k , the k th mode shape dominates there and the first singular u_{i1} is an estimate of the k th mode shape, i.e., $\hat{\phi}_k = u_{i1}$. Meanwhile, the corresponding singular values are the auto-PSD function of the corresponding single degree of freedom (SDOF) system, according to Eq. (2). This PSD function is identified around the peak ω_k by comparing the mode shape estimate $\hat{\phi}_k$ with the singular vectors u_{i1} for the frequency lines around the peak. As long as a singular vector is found to have a high modal assurance criterion (MAC) value with $\hat{\phi}_k$, the corresponding singular value belongs to the SDOF density function.

3.3 Test of main span girder

In December 2004, when the construction of RYSB had been almost completed, ambient vibration test of the main span girder was carried out. The equipments used for the tests include accelerometers, signal cables, and data acquisition system with signal amplifier and conditioner. The signal conditioner unit is used to improve the quality of the signals by filtering undesired frequency content and amplifying the signal.

To better identify three-dimensional mode shapes of the bridge, a dense arrangement of measuring points on the bridge deck in the vertical and lateral directions was proposed. Measurement stations were located at every other suspender's anchorage on the deck. As a result, there were 90 measurement stations in total, including 45 stations on the upstream side and 45 stations on the downstream side, as shown in Fig. 2. Considering the lateral vibrations of the deck are almost the same on the upstream side and on the downstream side, only 45 stations were used on the upstream side to measure lateral vibration responses.

Twenty-two low frequency force-balanced accelerometers were used in the tests, of which 21 accelerometers were moveable, while one vertical accelerometer at the station 18 was fixed as the reference one. Seven setups were proposed to cover all planned measuring points on the bridge. The ambient vibration signals were simultaneously recorded for 30 minutes at all channels. Each set of data

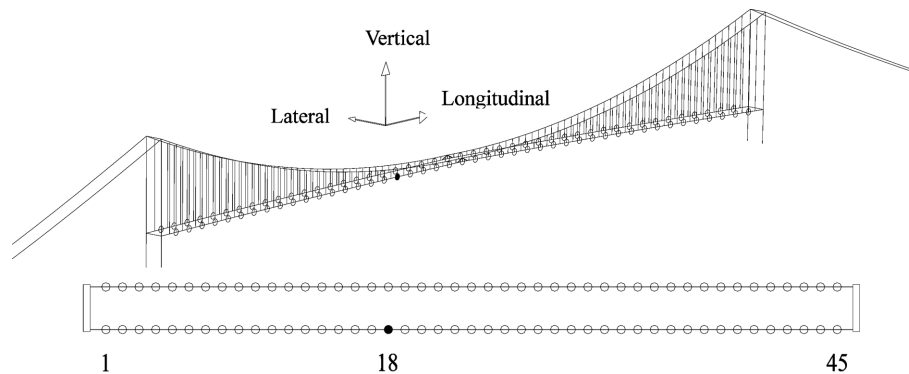


Fig. 2 Measurement points of main girder

Table 1 Identification results of modal frequency for the deck at different times

Order	Dec 21, 2004	Apr 22, 2005	Apr 23, 2005	May 2, 2005	Aug 6, 2005	Jan 7, 2006	Δf (%)	Mode shape
	TEST1 (5°C)	OMI1 (18°C)	OMI2 (21°C)	OMI3 (20°C)	OMI4 (26°C)	OMI5 (-2°C)		
L1	0.0635 (0.0586)	0.0634	0.0537	0.0517	0.0513	0.0519	22.6	1 st symmetric transverse
L2	0.1636 (0.1587)	0.1635	0.1379	0.1410	0.1367	0.1414	16.0	1 st asymmetric transverse
V1	0.1441	0.1440	0.1438	---	0.1000 (0.0800)	---	---	1 st asymmetric vertical
V2	0.1221	0.1227	0.1227	0.1227	0.1233	0.1227	0	1 st symmetric vertical
V3	0.1685	0.1672	0.1678	0.1672	0.1672	0.1666	0	2 nd symmetric vertical
V4	0.1880	0.1892	0.1880	0.1874	0.1868	0.1868	1.0	2 nd asymmetric vertical
T1	0.2417	0.2423	0.2428	0.2423	0.2417	0.2450	0	1 st symmetric torsion
T2	0.3077	0.3058	0.3058	0.3045	0.3040	0.3126	0.4	1 st asymmetric torsion

Note: ---: Not available $\Delta f = 100 \times (OMIS1 - OMIS3) / OMIS3$

was analyzed separately using aforementioned modal identification method to obtain mode shapes relative to the reference point (station 18). Mode shapes of the whole measurements could be synchronized according to the ratio to the same reference.

Some of identified frequencies of the girder are summarized in Table 1, referred as Test1. To evaluate the influence of temperature on variation of modal parameters, the corresponding daily-average temperature is also presented in Table 1. Measured modal shapes are illustrated in Fig. 3. The modal shapes calculated from the FEM developed in Section 5 are also shown in Fig. 3 for comparison. Most of the identified mode shapes are in good agreement with the results of FEM. However, it is worth noting that the frequencies of modes L1 and L2 can change during the test. So there are two values of L1 and L2 in Table 1. Moreover, the measured frequencies of modes L1, L2 and V1 are obviously higher than the design values illustrated in Table 3. According to the calculated results listed in section 5.2, it can be found that the frequencies of modes L1, L2 and V1 are sensitive to the boundary condition. The change of the expansion joints may lead to the changes of the frequencies of modes L1 and L2 during the test. Moreover, when the stiffness of the expansion joint is smaller, mode V1 is an

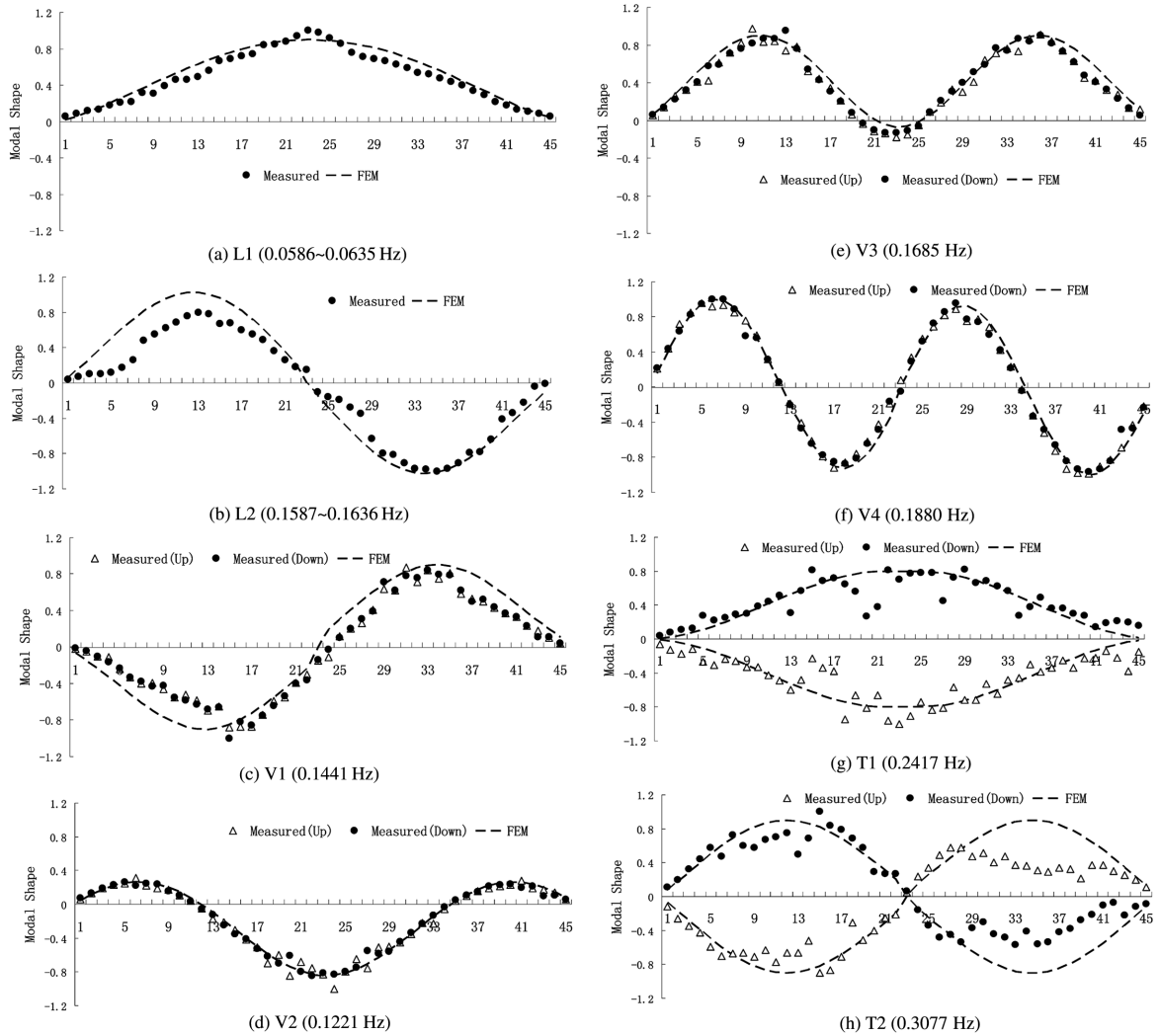


Fig. 3 Measured and calculated modal shapes

Table 2 Statistical value of the measured frequency and temperature

Order	Mean	Std dev	a	b	R^2
L1	0.0514	0.0008	-3E-5	0.0519	0.1387
L2	0.1398	0.0027	-2E-4	0.1417	0.3907
V2	0.1225	0.0003	-1E-6	0.1226	0.0019
V3	0.1874	0.0008	-3E-5	0.1877	0.2801
T1	0.2435	0.0013	-1E-4	0.2447	0.6807
T2	0.3100	0.0044	-4E-4	0.313	0.7110

asymmetric vertical mode with larger longitudinal movement, as shown in Fig. 4(a). When the stiffness of the expansion joint is larger, mode V1 is an asymmetric vertical mode without longitudinal movement, as shown in Fig. 4(b). Identification result of mode V1 shows that there are almost no

Table 3 Calculated results of the FEM under different boundary conditions

Order	Design value	Case 0	Case 1	Case 2		Case 3		
	Frequency (Hz)	Frequency (Hz)	Frequency (Hz)	$\Delta f1$ (%)	Frequency (Hz)	$\Delta f2$ (%)	Frequency (Hz)	$\Delta f3$ (%)
L1	0.0496	0.0495	0.0501	1.2	0.0544	9.9	0.0644	30.1
L2	0.1270	0.1291	0.1302	0.9	0.1381	7.0	0.1597	23.7
V1	0.0895	0.0885	0.1076	21.6	0.1356	53.2	0.1435	62.1
V2	0.1250	0.1242	0.1242	0.0	0.1244	0.2	0.1245	0.2
V3	0.1680	0.1689	0.1689	0.0	0.1689	0.0	0.1690	0.1
V4	0.1900	0.1883	0.1884	0.1	0.1889	0.3	0.1891	0.4
T1	0.2240	0.2315	0.2315	0.0	0.2315	0.0	0.2315	0.0
T2	0.2810	0.2936	0.2936	0.0	0.2940	0.1	0.2952	0.5

Note: Case0: expansion joints stiffness $k = 0$ kN/m; Case1: expansion joints stiffness $k = 1.0 \times 10^2$ kN/m; Case2: expansion joints stiffness $k = 1.0 \times 10^3$ kN/m; Case3: expansion joints stiffness $k = 1.0 \times 10^4$ kN/m; $\Delta f1 = 100 \times (\text{Case1} - \text{Case0})/\text{Case0}$, $\Delta f2 = 100 \times (\text{Case2} - \text{Case0})/\text{Case0}$, $\Delta f3 = 100 \times (\text{Case3} - \text{Case0})/\text{Case0}$

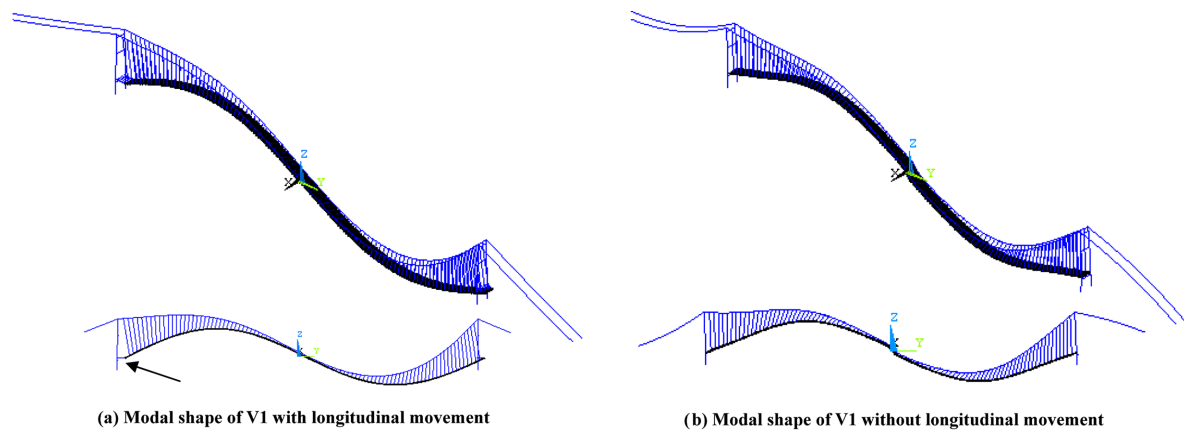


Fig. 4 Calculated modal shape of V1 with different expansion joint stiffness

movements in the longitudinal direction, which is consistent with the calculated result of FEM with a larger stiffness of the expansion joint.

4. Study in variation of modal parameters based on SHMS

4.1 Structural health monitoring system

To monitor the performance and health status of the bridge, a structural health monitoring system (SHMS) has been installed on the RYSB (Li *et al.* 2003). The SHMS consists of sensor system, data acquisition system, data communication and transmitting system, and data processing and analysis system. The sensor system consists of a wide range of analog sensors, including accelerometers, anemometers, strain gauges, displacement sensors, temperature sensors, global position system (GPS),

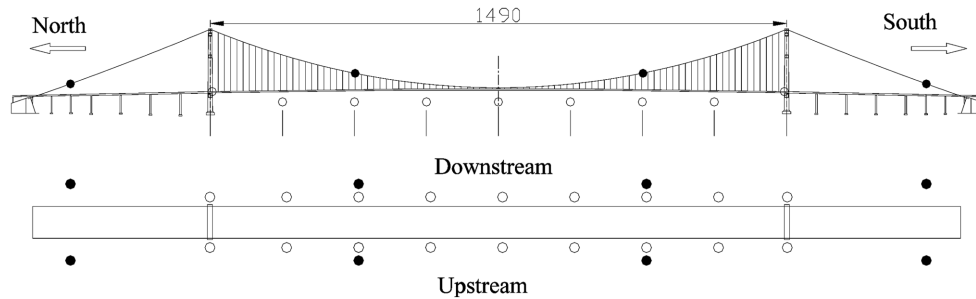


Fig. 5 Layout of accelerometers in SHMS of the RYSB

etc. Temperature sensors were installed on the girders to measure the temperatures of steel and atmosphere.

The layout of accelerometers in the SHMS of RYSB is shown in Fig. 5. There are 4 sections on the main cables, including 8 lateral accelerometers and 4 vertical accelerometers. A total of 29 accelerometers are located at the 9 sections of the bridge deck in the main span. A total of 12 accelerometers have been installed in the north tower and the south tower, respectively. The total number of accelerometers is 65. Accelerometers convert the ambient vibration responses into electrical signals. Then the signal conditioner unit is used to improve the quality of these signals by filtering undesired frequency contents and amplifying the signals. The filter frequency is 10 Hz, and the amplify factor is about 1000.

4.2 Application of OMI

Based on the SHMS and the aforementioned output-only identification methods, an operational modal identification (OMI) program is compiled, which is used to extract the modal parameters in an online manner.

To study the variation of modal parameters at different times, a large amount of vibration data from April 2005 to February 2006 were analyzed. Some identified modal parameters in typical or special cases are summarized in Table 1. The bridge was opened to traffic on May 1st, 2005. Modal parameters identified before the bridge opened to traffic were selected on 22 April and 23 April 2005, referred as OMI-1 and OMI-2, respectively. The results identified in traffic were selected on 2 May 2005, 6 August 2005 and 7 January 2006, referred as OMI-3, OMI-4 and OMI-5, respectively.

As an example, the vibration response data recorded during the excitation of typhoon Matsa on 6 August 2005 is used to illustrate the application of operational modal identification program. The excitation level of typhoon vibration is much higher than that of ambient vibration. Figs. 6 and 7 show the average normalized power spectral density function (ANPSD) of the vertical and lateral vibration responses of girders, respectively. The frequencies of 0.2417 Hz and 0.3040 Hz correspond to torsional modes, as shown in Table 1, which have movements on both the vertical and lateral directions. Namely, the vertical and lateral vibrations of the girder are coupled as shown in Figs. 6 and 7. All the PSDs have well-separated spectral peaks in the frequency range of 0 to 0.5 Hz and a remarkable consistency in their occurrences. Generally, the data of vertical response are good and with almost no influences of noise. But the data of lateral response are worse than those of vertical response, especially when the wind speed is low.

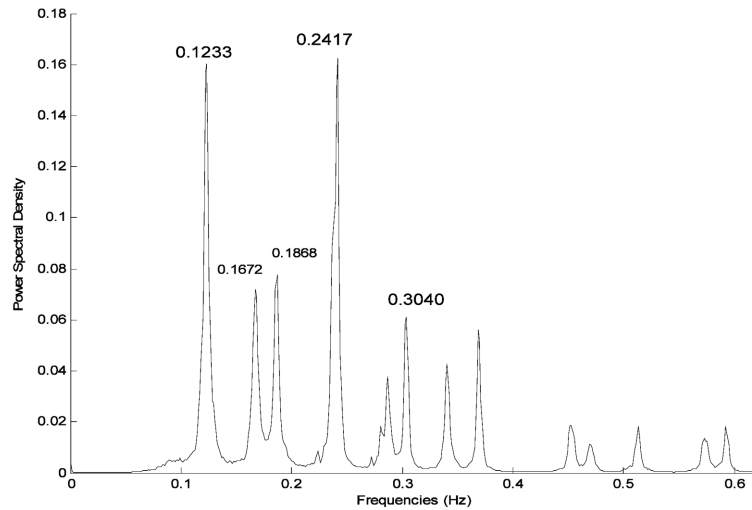


Fig. 6 ANPSD of deck vertical vibration data

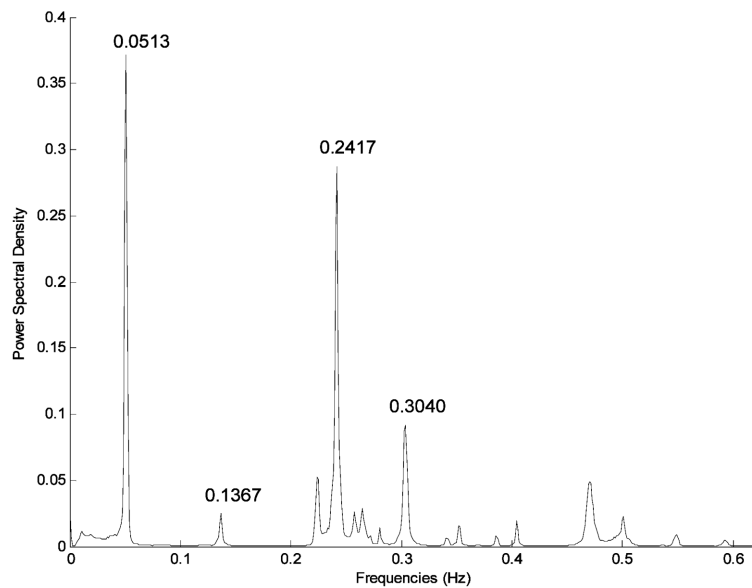


Fig. 7 ANPSD of deck lateral vibration data

4.3 Variation of modal frequency before and after the bridge opened to traffic

Comparing the results identified before the bridge opened to traffic, referred to TEST1, OMI-1 and OMI-2, it is observed that the frequencies of the modal shapes L1 and L2 may have a significant change in a short time. From 22 April to 23 April 2005, the frequencies of mode L1 and L2 vary from 0.0634 Hz and 0.1635 Hz to 0.0537 Hz and 0.1379 Hz, respectively. The frequency of mode V1 has almost decreases, which can be identified at 0.1440 Hz for OMI-2, as shown in Fig. 8. After the bridge opened to traffic, the frequencies of L1 and L2, referred to OMI-3 to OMI-5, have almost no decreases. However, mode V1 with a frequency at 0.1440 Hz can not be identified, as shown in Fig. 9. In fact, the

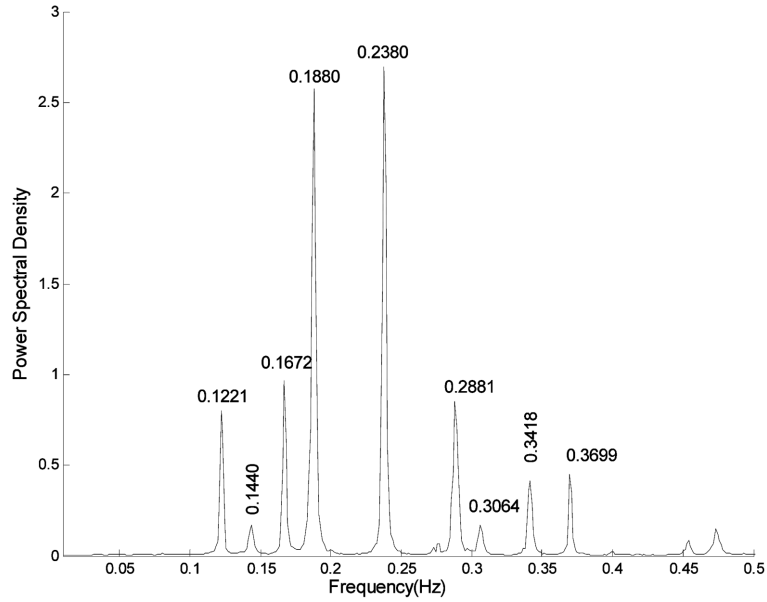


Fig. 8 Spectra of the vertical vibration response in April 2005

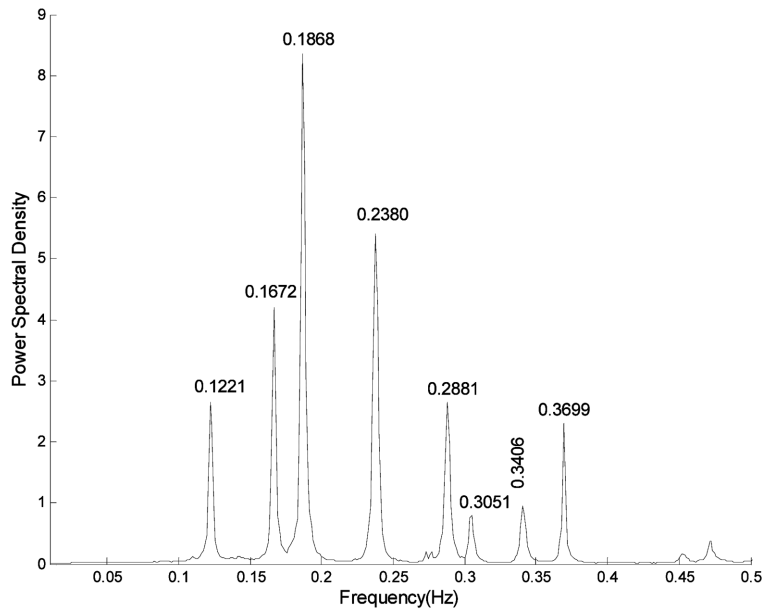


Fig. 9 Spectra of the vertical vibration response in May 2005

mode V1 has become a new mode with longitudinal movement. Moreover, it is difficult to identify its frequency from vertical vibration responses under small excitations. When the bridge experiences a strong excitation, such as typhoon excitation, the new mode V1 can be identified with the frequency between 0.08 Hz and 0.1 Hz. Except for modes V1, L1 and L2, other modes have almost no change in frequencies.

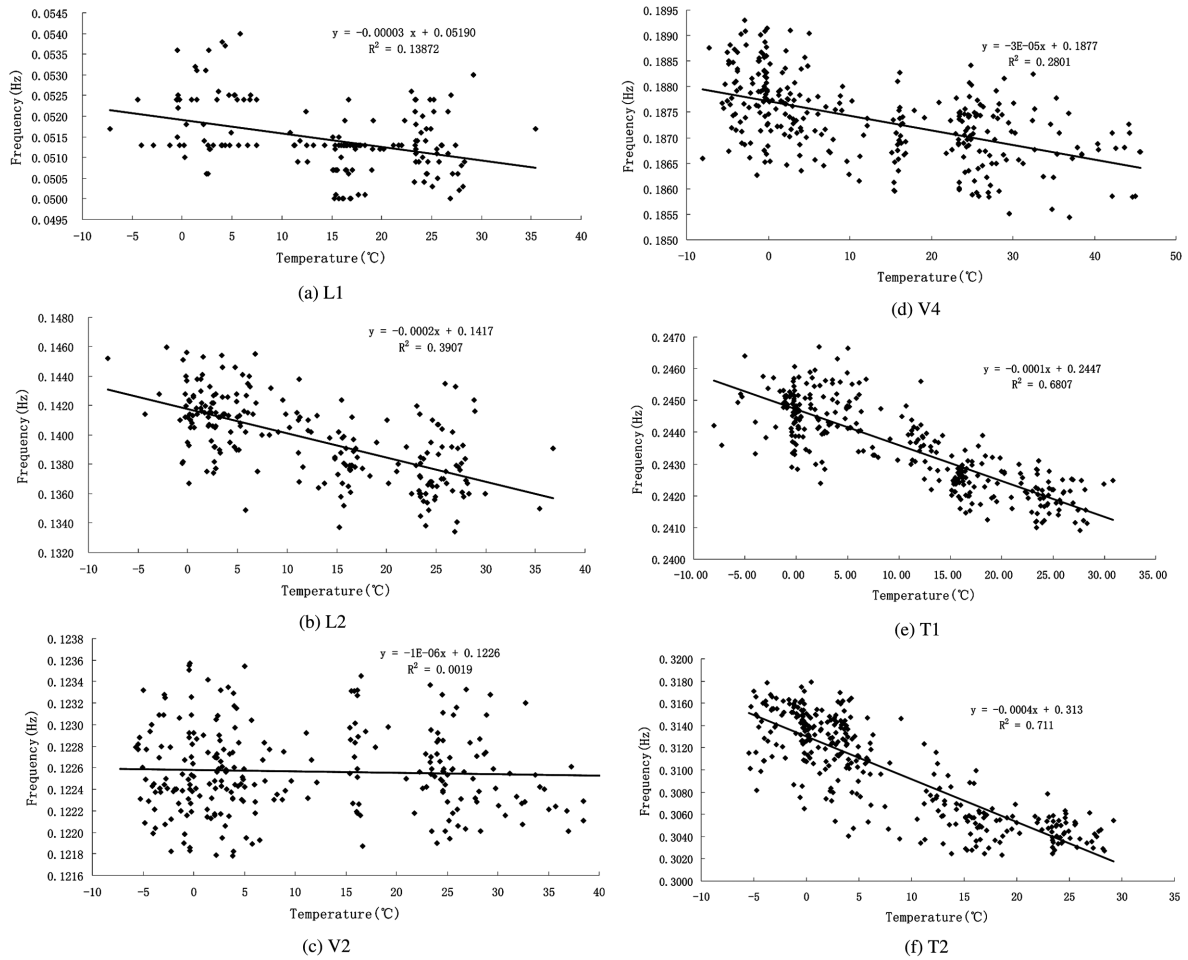


Fig. 10 Identified modal frequencies under different temperature

4.4 Variation of modal frequency with temperature

It is well known that temperature may have an effect on the natural frequencies of large civil structures. In order to evaluate the influence of temperature on modal parameters, a set of vibration data monitored from May 2005 to February 2006 is used to extract modal parameters in different temperatures. Monitored data of three hundred days were finally selected for the regression analysis. Fig. 10 shows the variability of the frequencies of modes L1, L2, V2, V4, T1 and T2 with temperatures from -10 °C to 40 °C. Because the frequency of mode V1 is difficult to obtain, there are no statistical results for mode V1. It can be seen from Fig. 10 that the natural frequencies have a slow downward trend as temperature increases. Linear regression is used to model the relationship between the frequency and temperature. This relationship is described in the following formula

$$f = a\Delta T + b \tag{4}$$

The coefficients of the linear equation estimated are listed in Table 2, where R^2 is the squared value of the correlation coefficient. The regression functions between the frequencies of modal shapes L1 and

L2 and temperature can be expressed as

$$f_{L1} = -0.00003\Delta T + 0.0519(\text{Hz}) \quad (5)$$

$$f_{L2} = -0.0002\Delta T + 0.1417(\text{Hz}) \quad (6)$$

If temperature increases by 10 °C, the frequencies of L1 and L2 decrease by 0.6% and 1.4%, respectively. In the case of OMI-1 and OMI-2, the variation of current temperature is only about 3 °C. Therefore, the influence of temperature on the frequencies of modes L1 and L2 is negligible. Other effects, e.g., boundary conditions, which may cause significant variations in modal frequencies, should be considered.

5. Dynamic analysis of parameter variations based on finite element model

Comparisons of modal parameters show that the first three modal frequencies experience significant changes. Also, the correlation analysis between measured modal parameters and the temperature show that temperature has a slight influence on the first order modal frequencies. In order to account for the significant changes, a three-dimensional FE model is developed by using the FE software ANSYS to analyze sensitivities of parameter variations to boundary conditions and vehicle loads. Other factors, such as the material and structural properties, are also considered.

5.1 Finite element model of RYSB

The 3-D finite element model of the RYSB is developed with the following assumptions:

- (1) The cables are modeled by the 3-D tension-only truss elements (LINK10 element in ANSYS), and the pre-tensions of the cables are incorporated by the initial strains. A suspension structure has a unique initial equilibrium configuration at a certain temperature due to dead load. Thus, the initial equilibrium configuration is the starting position to perform the subsequent analysis. Meanwhile, the internal forces due to dead load are dominant in all structural components. Therefore, the calculation of this initial equilibrium configuration is necessary in the finite element modeling of suspension bridges.
- (2) The towers are modeled as the 3-D elastic beam elements (BEAM4 element in ANSYS). At the column-beam joints of towers, rigid arms are added at the ends of the beam elements to deal with the node-rigid-zone problems, which arise from the spatial effects of concrete box structures. The sensitivity-based model updating technique is used to update the finite element model of bridge towers according to measured frequencies from ambient vibration test of towers.
- (3) The steel girder is modeled by shell elements (SHELL63 element in ANSYS). An orthotropic shell element is chosen to model the bridge deck in the global-level model by simplifying the U-shaped longitudinal ribs only. In this way, it keeps the spatial box configuration to make the computation more accurate. The principles are listed as follows: ① The mass distribution of the equivalent bridge deck using orthotropic shell elements should be equal to the original one. ② The axial, vertical and lateral stiffness of the orthotropic shell elements should be equal to the actual deck plates, thus it can ensure the bending stiffness of entire steel-box-girder is equivalent to the original one. ③ The shear stiffness of the orthotropic shell elements should be equal to the actual deck plates to guarantee the torsion stiffness of entire steel-box-girder is equivalent to the original one. The entire bridge model is also updated according to the measured frequencies.

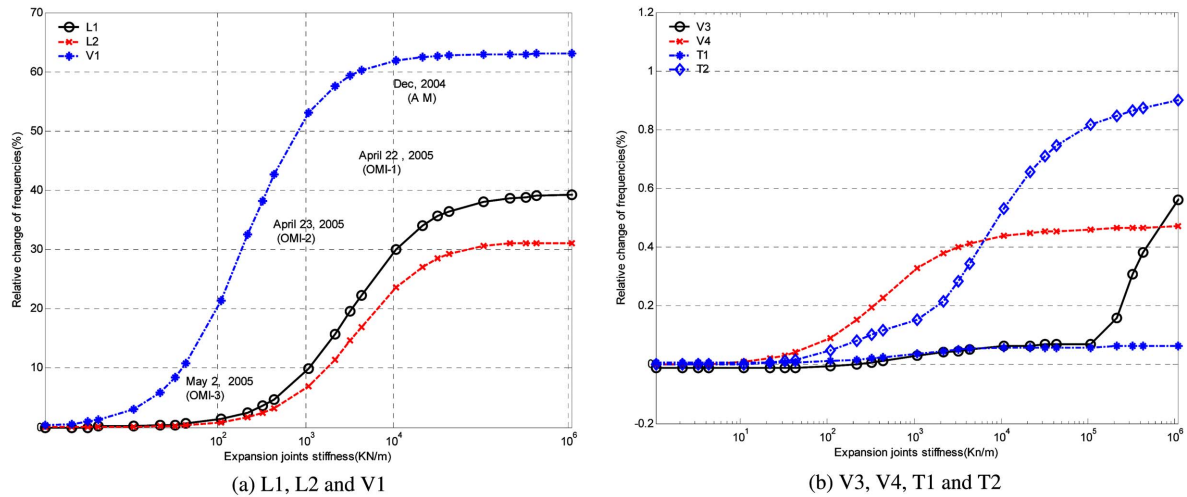


Fig. 11 Variation of frequencies with the stiffness of expansion joints

5.2 Effects of expansion joints on modal frequencies

Expansion joints at two ends of main girder are important components in bridge structures. They are used to accommodate bridge movements due to creep and shrinkage of concrete, temperature fluctuations and traffic loadings (Ni *et al.* 2007). However, the stiffness of expansion joints is usually ignored in bridge design. To obtain exact dynamic parameters, the longitudinal restraint action of bridge deck arising from the anti-push rigidity of expansion joints and the friction of bearing is simulated by one-dimensional longitudinal spring elements (COMBINE14 element in ANSYS). Considering that the stiffness of the expansion joint is time-dependent and difficult to determine, the natural frequencies with different spring stiffness are calculated.

A total of 25 cases corresponding to the stiffness from 0 *KN/m* to 1E6 *KN/m* are calculated. The variations of frequencies with respect to the stiffness of expansion joints are illustrated in Fig. 11. It can be seen from Fig. 11(a) that frequencies of modes V1, L1 and L2, are sensitive to the boundary conditions of the girder ends. When the stiffness of expansion joints varies from 10 *KN/m* to 1E4 *KN/m*, the frequency of mode V1 increases by almost 60%. For the stiffness of expansion joints varying from 100 *KN/m* to 1E5 *KN/m*, the frequencies of modes L1 and L2 increase by 40% and 30%, respectively.

From Fig. 11(b), it is observed that the stiffness of expansion joints has very small influences on the frequencies of other modes, such as V3, V4, T1 and T2. The maximum relative change of these frequencies is less than 1%.

Table 3 lists the results of four typical cases with the design values provided by the bridge designer. The stiffness of expansion joints is not included in the model provided by the bridge designer, so its boundary condition corresponds to the Case0. The good agreement between design values and Case0 demonstrates that the model developed in the paper is reliable. In the case of Case1, the stiffness of expansion joints takes the value of 1.0×10^2 *kN/m*. The calculated modal parameters of all order can best fit the measured results after the bridge opened to traffic. In the Case2, stiffness of expansion joints takes the value of 1.0×10^3 *kN/m*, and the calculated modal parameters of all order can best fit the measured results before the bridge opened to the traffic. In the Case3, stiffness of expansion joints takes the value of 1.0×10^4 *kN/m*, and the calculated results can best fit the results measured when the bridge

Table 4 Calculated results of the FEM under different vehicles

Order	Case0	Case1		Case2	
	Frequency (Hz)	Frequency (Hz)	$\Delta f1$ (%)	Frequency (Hz)	$\Delta f2$ (%)
L1	0.0608	0.0606	-0.3	0.0604	-0.7
L2	0.1515	0.1508	-0.5	0.1501	-0.9
V1	0.1421	0.1417	-0.3	0.1413	-0.6
V2	0.1245	0.1242	-0.2	0.124	-0.4
V3	0.1690	0.1686	-0.2	0.1683	-0.4
V4	0.1890	0.1888	-0.1	0.1885	-0.3
T1	0.2315	0.2303	-0.5	0.229	-1.1
T2	0.2946	0.2926	-0.7	0.2908	-1.3

Note: $\Delta f1 = 100 \times (\text{Case1} - \text{Case0}) / \text{Case0}$, $\Delta f2 = 100 \times (\text{Case2} - \text{Case0}) / \text{Case0}$

was newly built, i.e., the values for the column of TEST1 in Table 1. From Fig. 11(a), the stiffness of expansion joints corresponding to the different measurement times can be decided.

When the bridge was newly built, the expansion joints remain stuck, resulting in a higher stiffness. Learned from Fig. 11(a), the stiffness of expansion joints is nearly 1.0×10^4 kN/m. The frequencies of L1, L2 and V1 measured during December 2004 (referred to TEST1) and 22 April 2005 (referred to OMI-1) are obviously higher than the design values listed in Table 3. After the bridge has been used for some time, its stiffness begins to decrease sharply. When the stiffness of expansion joints varies from 1.0×10^4 kN/m to 1.0×10^3 kN/m, the frequencies of L1 and L2 have higher decreases than the change of V1. Therefore, the frequencies of L1 and L2 extracted on OMI-1 and OMI-2 have obvious decreases but the frequency of V1 has a small change. When the stiffness of expansion joints varies from 1.0×10^3 kN/m to 1.0×10^2 kN/m, the frequency of V1 has larger decrease than the changes of L1 and L2. So the frequency of V1 extracted after the bridge to traffic, such as OMI-3, OMI-4 and OMI-5 has an obvious decrease but the frequencies of L1 and L2 have small changes.

The mode V1 calculated from FEM is an asymmetric vertical vibration shape with longitudinal floating. The movement in the longitudinal direction decreases with the increase of the stiffness of expansion joints. However, the measured mode shape of V1 before the bridge opened to traffic has almost no movements in the longitudinal direction, which indicates the stiffness of expansion joints at that time is higher. The model used in design stage assumes a hinge connection between towers and girders to allow rational and longitudinal movements. Therefore, the stiffness of the expansion joints was ignored, and the calculated frequencies of the low-order modal shapes would be underestimated greatly. The boundary conditions of bridge deck should be modeled appropriately.

5.3 Effects of vehicle loads on modal frequencies

The influence of vehicle loads on modal parameters is investigated based on the 3-D finite element model. Vehicles are simulated by mass elements (MASS21 element in ANSYS). According to the statistical daily traffic flow provided by the management of the bridge, two cases are calculated. Case1 adds mass elements with $4.5E5$ Kg, corresponding to 45 vehicles to the finite element model. Case2 adds mass elements with $9.0E5$ Kg, corresponding to 90 vehicles to the finite element model. Calculated modal parameters of the two cases are summarized in Table 4, which shows that variations of modal parameters due to vehicle loads are negligible.

Table 5 Material properties of the RYSB

Group number	Name	Young's modulus (MPa)	Poisson's ratio	Mass density (kg/m ³)	Structural member
1	E_D	2.10E5	0.3	7850	Deck
2	E_C	2.00E5	0.3	7850	Cables
3	E_T	3.45E4	0.2	2500	Tower

Table 6 Calculated frequencies with different material properties

Order	Case0	Case1		Case2		Case3	
	Frequency (Hz)	Frequency (Hz)	$\Delta f1$ (%)	Frequency (Hz)	$\Delta f2$ (%)	Frequency (Hz)	$\Delta f3$ (%)
L1	0.0495	0.0497	0.4	0.0506	2.2	0.0506	2.2
L2	0.1291	0.1305	1.1	0.1381	7.0	0.1381	7.0
V1	0.0885	0.0886	0.1	0.0907	2.5	0.0907	2.5
V2	0.1242	0.1243	0.1	0.1272	2.4	0.1272	2.4
V3	0.1689	0.1689	0.0	0.1729	2.4	0.1730	2.4
V4	0.1883	0.1885	0.1	0.1928	2.4	0.1928	2.4
T1	0.2315	0.2320	0.2	0.2358	1.9	0.2364	2.1
T2	0.2936	0.2960	0.8	0.2994	2.0	0.2995	2.0

Note: Case0: The designed material properties; Case1: $1.05 \times E_D$; Case2: $1.05 \times (E_D + E_C)$; Case3: $1.05 \times (E_D + E_C + E_T)$; $\Delta f1 = 100 \times (\text{Case1} - \text{Case0}) / \text{Case0}$, $\Delta f2 = 100 \times (\text{Case2} - \text{Case0}) / \text{Case0}$, $\Delta f3 = 100 \times (\text{Case3} - \text{Case0}) / \text{Case0}$

5.4 Effects of material properties on modal frequencies

Basic materials used in the Run Yang Suspension Bridge are structural steel, concrete and steel cable. The material parameters are summarized in Table 5.

To study the effect of material properties on the frequency of the suspension bridge, a total of 4 cases with different Young's modulus are calculated. As listed in Table 6, it can be found that the frequencies of all modes are sensitive to the properties of the cable. If the parameter E_C increases by 5%, most of frequencies increase by about 2.5%. The frequency of mode L2 has an increase of 7%. However, the differences between the designed properties and their real values are much less than 5%. In this regard, material property is not the main effect to the differences between the measured and analyzed frequencies.

6. Conclusions

Identification results of actual modal frequencies of the Run Yang Suspension Bridge under different conditions are investigated based on ambient vibration tests and the structural health monitoring system. Some low-order modal frequencies have obvious variations before and after the bridge opened to traffic. These significant changes imply that the bridge may experience the "re-accommodation" after the completion of the bridge. The correlation analyses between measured modal parameters and the temperature show that temperature has a slight influence on low-order modal frequencies. Analyses

based on the finite element model indicate that the variability of expansion joint stiffness can lead to significant changes in the low-order modal frequencies and has almost no influence on the frequencies of other mode shapes. Therefore, it can be concluded that the observed changes on modal parameters are mainly due to boundary condition effects of the bridge and not due to temperature or other loading. The boundary conditions have a significant influence on the low-order modal parameters of the suspension bridge.

Acknowledgements

The work presented in this paper was supported by the National Outstanding Young Scientists' Foundation of China under Grant No. 50725828, the Key Projects in the National Science & Technology Pillar Program of China (No. 2006BAJ03B05) and the Southeast University Outstanding Doctoral Foundation.

References

- Brincker, R., Zhang, L.M. and Andersen, P. (2001), "Modal identification of output-only systems using frequency domain decomposition", *Smart Mater. Struct.*, **10**(3), 441-445.
- Fujino, Y. and Siringoringo, D.M. (2007), "Vibration-based health monitoring of bridges and transportation infrastructures", *Proceedings of the 2nd International Conference on Structural Condition Assessment, Monitoring and Improvement (SCAMI-2)*, China, November.
- Gentile, C. and Gallino, N. (2008), "Ambient vibration testing and structural evaluation of an historic suspension footbridge", *Adv. Eng. Softw.*, **39**(4), 356-366.
- He, X.F., Moaveni, B., Conte, J.P., Elgamal, A. and Masri, S.F. (2009), "System identification of Alfred Zampa Memorial Bridge using dynamic field test data", *J. Struct. Eng.-ASCE*, **135**(1), 54-66.
- Ko, J.M., Chak, K.K., Wang, J.Y., Ni, Y.Q. and Chan, T.H.T. (2003), "Formulation of an uncertainty model relating modal parameters and environmental factors by using long-term monitoring data", *Proc. SPIE*, **5057**, 298-307.
- Ko, J.M. and Ni, Y.Q. (2005), "Technology developments in structural health monitoring of large-scale bridges", *Eng. Struct.*, **27**(12), 1715-1725.
- Li, A.Q., Miao, C.Q., Li, Z.X., Han, X.L., Wu, S.D., Ji, L. and Yang, Y.D. (2003), "Health monitoring system for the Run Yang Yangtse River Bridge", *J. Southeast Univ. (Natural Science Edition)*, **33**(5), 544-548.
- Magalhaes, F., Cunha, A. and Caetano, E. (2008), "Dynamic monitoring of a long span arch bridge", *Eng. Struct.*, **30**(11), 3034-3044.
- Ni, Y.Q., Hua, X.G., Wong, K.Y. and Ko, J.M. (2007), "Assessment of bridge expansion joints using long-term displacement and temperature measurement", *J. Perform. Constr. Fac.*, **21**(2), 143-151.
- Ren, W.X., Blandford, G.E. and Harik, I.E. (2004), "Roebling suspension bridge. I: finite-element model and free vibration response", *J. Bridge Eng.*, **9**(2), 110-118.
- Sohn, H., Dzwonczyk, M., Straser, E.G., Kiremidjian, A.S., Law, K.H. and Meng, T. (1999), "An experimental study of temperature effect on modal parameters of the Alamosa Canyon Bridge", *Earthq. Eng. Struct. D.*, **28**(8), 879-897.